RSC Advances

ROYAL SOCIETY OF CHEMISTRY

www.rsc.org/advances

Submit to: RSC Advances

Paper type: Full paper

Title: Commercial potato protein concentrate as a novel source for thermoformed bio-based plastic films with unusual polymerization and tensile properties

William R. Newson[a]*, Faiza Rasheed[a], Ramune Kuktaite[a], Mikael S. Hedenqvist[b], Mikael Gällstedt[c], Tomás S. Plivelic[d], Eva Johansson[a]

a Department of Plant Breeding, The Swedish University of Agricultural Sciences, SE-230 53 Alnarp, Sweden

b Department of Fibre and Polymer Technology, Royal Institute of Technology, SE-10044 Stockholm, Sweden

c Innventia AB, Box 5604, SE-11486 Stockholm, Sweden

d MAX IV Laboratory, Lund University, Box 118, SE-221 00 Lund, Sweden

* Corresponding Author

*William R. Newson, Department of Plant Breeding, Swedish University of Agricultural Sciences, SE-230 53 Alnarp, Sweden

Phone: +46 40 415344.

Fax: +46 40 415519.

e-mail: bill.newson@slu.se

Abstract

Commercial potato protein concentrate (PPC) was investigated as a source of thermoformed bio-based plastic film. Pressing temperatures of 100 to 190^{o}C with 15 to 25% glycerol were used to form PPC films. The shape of the tensile stress-strain curve in thermoformed PPC was controlled by glycerol level and was independent of processing temperature. Tensile testing revealed that elongation at break increased with processing temperature while Young's modulus was unaffected by processing temperature, both in contrast to previous results in protein based systems. Also in contrast to previous studies, Young's modulus was found to be only sensitive to glycerol level. Maximum tensile stress increased with increasing processing temperature for PPC films. Maximum stress and strain at break correlated with the extractable high molecular weight protein content of the processed films measured with size exclusion chromatography. Infrared absorption indicated that the content of β-sheet structure increased from the commercial protein concentrate to that pressed at 100 ^{o}C, but did not further develop with increasing press temperature. Changes in structural arrangements were observed by small angle x-ray scattering indicating the development of different correlation distances with processing temperature but with no clear long range order at the supramolecular level. The novel Young's modulus behaviour appears to be due to constant secondary structure or the effect of aggregated protein structure formed during protein production. Unique strain at break behaviour with processing temperature was demonstrated, likely due to new connections formed between those aggregates.

Introduction

The use of protein co-products from various industrial processes for making materials is of interest due to environmental concerns and the security of petroleum supplies. Potato protein concentrate (PPC), a co-product of the industrial potato starch industry, is available in large quantities at a reasonable price of 1.4-1.5 €/kg, and is therefore an interesting source for bio-based materials. Potato protein concentrate is extracted from potato fruit water (PFW), a co-product of industrial potato starch production, having approximately 5% dry matter with one third of this being proteins, peptides and amino acids[1]. The remainder contains other soluble potato components and a reducing agent, such as $NaHSO_3$, used to prevent starch browning. During the commercial production of PPC from PFW the conditions for protein coagulation are: pH of 3.5-5[1] a temperature of 75 to 120°C[2] followed by spray drying[1]. Although this treatment leaves the proteins denatured both chemically and thermally, it is required to induce protein coagulation for commercially viable protein recovery.

Potato protein concentrate consists of two main protein groups, patatin (molecular weight 40-43 kDa, 40-60% of total protein)[3, 4], three classes of protease inhibitors (8-25 kDa, 20-50%)[3, 4] as well as other mostly higher molecular weight proteins (e.g. 80 kDa phosphorylase, 20-30%)[3] . The overall amino acid profile of PPC is low in sulphur containing amino acids, but is relatively high in lysine[5]. Patatin and the protease inhibitors are well characterized for their crystalline structure and biological function.[6-9] However, thermal/acid coagulation during protein recovery denatures the proteins and effectively deactivates their enzymatic activity[1]. During this acidic thermal processing there also exists possible reactions with phytochemicals such as phenolics resulting in protein cross-linking[10] or deactivation of reactive amino acids such as lysine[11].

Protein based materials are mainly of interest as films, processed in the presence of a plasticizer such as glycerol to improve flexibility[12-25]. Plant protein films have demonstrated attractive oxygen and CO_2 barrier properties for proteins such as soy[25], wheat gluten[12] and corn zein[26] among others,

while their mechanical properties need to be increased to compete with petrochemically based polymers.

Despite availability and reasonable cost, to our knowledge potato protein has not been considered before as a possible main source for protein based materials. So far, potato protein has formed a minor component in potato peel waste based materials (16 g protein/100g)[13] and has been used as a minor addition (5%) to carboxylated acrylonitrile-butadiene rubber[27]. In the former case, glycerol and lecithin were used to act as plasticizers and emulsifiers, respectively, and high pressure homogenization was most effective in producing solutions for cast films. In the latter case, potato proteins acted to increase crosslink density of vulcanizates and consequently improved mechanical properties, while simultaneously increasing biodegradability[27].

Chemical and thermal denaturation during protein based material processing unfolds proteins exposing amino acid reactive groups. This unfolding makes reactive functional groups available for covalent bonding such as disulphide and isopeptide bonds, increases protein-protein interactions[28] and Maillard reactions with saccharides[1, 28]. Chemical cross linkers, such as formaldehyde and glutaraldehyde, can be used to form inter-protein covalent bonds resulting in improved protein networks, but are criticized for their poor environmental footprint[29]. Denaturation during processing can facilitate refolding into protein secondary structures, such as β-sheets, contributing to improved material properties[19, 20]. Thermally processed wheat gluten based materials with improved mechanical properties[14] and gas permeability[19] have been found to have superstructural protein arrangements using small angle x-ray scattering (SAXS)[15, 18] . Thermal processing in protein based materials results in a more developed network structure with higher stiffness and lower elongation to break as the processing temperature increases[16, 17]. At higher temperatures the thermal damage of proteins becomes the dominant factor and the protein network begins to degrade[17, 30].

By examining changes in protein polymerization behaviour through solubility via size exclusion high performance chromatography (SE-HPLC)[15, 17, 18] and protein structural organization via both SAXS[15, 18]

and infrared spectroscopy (IR)[15, 18], relationships between processing conditions and structure-property relationships of protein based material can be explored.

The aim of this study was to examine the suitability of commercial potato protein for bio-based films. We also aimed to examine the effect of plasticization and thermal processing on the mechanical properties of protein based materials, as well as explore the underlying changes governing these properties. The relationship between the tensile properties and protein network was probed via SE-HPLC measurements, while the effect of protein structural organization was examined through IR and SAXS.

Materials and Methods

Materials

Commercial PPC, protein content 82% ±2 (Dumas method, Flash 2000 NC Analyzer, Thermo Scientific, USA, NX6.25), moisture content 8.1% ±0.4, (dry basis, dried 105 °C, 3 h) was graciously provided by Lyckeby Starch AB (Sweden) and used as received.

Compression moulding

Compression moulding was performed as in Newson et al. [17] Briefly, PPC and glycerol (99.5%, Karlshams Tefac, Sweden) were mixed by hand using a mortar and pestle until the glycerol was evenly distributed (3-5 min). The mixture was placed between preheated aluminium plates with polyethylene terephthalate release film in the centre of a 100 mm X 100 mm opening in a 0.5 mm thick aluminium frame to control the size and thickness of the film. A 100 kN moulding force was applied for 5 min to all samples. The films were subsequently cooled in the frame between two room temperature aluminium plates.

Tensile testing

Tensile testing was carried out as in Newson et al.[17] Briefly, tensile specimens were punched from PPC films (ISO 37-type 3, Elastocon, Sweden) and conditioned for 48 h at 23˚C and 50% relative humidity (RH) before testing. Thickness was measured on each specimen at 5 locations in the test section (indicator IDC 112B with stand, Mitutoyo, Sweden) and averaged. The specimens were tested with an Instron 5566 universal test machine and data collected using Bluehill software (Instron, Sweden) at 23˚C and 50% RH using 30 mm clamp separation, crosshead speed of 10 mm/min and a 100 N load cell. Stress was calculated from the applied force divided by the cross sectional area of the reduced width section while strain was calculated from the crosshead

displacement divided by length of the reduced width section, Young's modulus (E-modulus) was calculated according to ASTM D638[31]. All values are from a minimum of 5 replicates.

Water absorption

Water absorption tests were carried out based on Newson et al.[32] Three replicate samples were prepared from the potato protein films with a 5 mm diameter punch and lyophilized for a minimum of 48 h (Scanvac Coolsafe, Scanlaf, Denmark), weighed and immersed in water for 24 h at 4^{o}C to prevent microbial growth. Disks were removed from the water, held vertically for 10 s, the pendant drop removed and then blotted between dry filter paper (grade 1701, Munktell, Sweden) under a 25 g weight for 10 s and weighed. The samples were again lyophilized and weighed. The water absorption was calculated according to the following formula (swollen mass - final lyophilized mass)/final lyophilized mass and mass loss during immersion as (original lyophilized mass – final lyophilized mass)/final lyophilized mass.

Size exclusion high performance liquid chromatography

To determine the protein solubility and size distribution of the extractable proteins in PPC films a procedure similar to the three-step extraction developed by Gällstedt *et al.*[12] was used. Briefly, samples of each film were reduced in size by hand cutting, to approximately 0.2 mm and 16.5 (±0.05) mg was weighed into 1.5 ml centrifuge tubes (in triplicate). All extractions were carried out serially in 1.4 ml extraction buffer (0.5% (wt/vol) SDS (Duchefa, Netherlands), 0.05M NaH_2PO_4 (Baker, Netherlands), pH 6.9) as follows; extraction 1, vortexing for 10 seconds, shaking 5 minutes at 2000 rpm; extraction 2, 30 seconds ultrasonication at an amplitude of 5 µm (Sanyo Soniprep, Tamro, Sweden); extraction 3, 30 + 60 seconds ultrasonication at the same amplitude. After each extraction

the sample was centrifuged at 19000 RCF for 30 minutes and the supernatant decanted directly into HPLC vials.

Chromatography was performed on a Waters 2690 Separations Module and Waters 996 Photodiode Array Detector (Waters, USA) at an isocratic flow of 0.2 ml/min (50% Acetonitrile (Merck, Germany), 0.1% trifluroacetic acid (TFA, spectroscopy grade, Merck); 50% H_2O (Millipore, USA), 0.1% TFA). A 20 µl injection of supernatant was separated through a prefilter (SecurityGuard GFC 4000, Phenomenex, USA) and main column (Biosep-SEC-S 4000 300mm X 4.5mm, Phenomenex). Data was 3D blank extracted using the extraction buffer and chromatograms extracted at 210 nm and integrated into 2 arbitrary fractions; high molecular weight (HMw) from 7.5 to 14 minutes and low molecular weight (LMw) from 14 to 30 minutes using Empower Pro software (Waters, USA). The areas of the elution intervals were normalized to the total area of the chromatograms for protein extraction of as-received PPC and corrected for glycerol content.

Small angle X-ray scattering

The small angle X-ray scattering (SAXS) experiments were carried out at beamline I911-4 of the MAX-IV Laboratory, Lund, Sweden[33]. A monochromatic beam with a 0.91 Å wavelength was used with a sample to detector distance of 1901.71 mm and an exposure time of approximately 5 minutes for each sample. Two dimensional data was obtained with a hybrid pixel x-ray detector (Pilatus 1M, Dectris, Switzerland). The software program bli9114 was used for analysis of X-ray scattering data[33]. Average radial intensity profiles were obtained as a function of the scattering vector q ($q = 4\pi/\lambda \sin(\theta)$, where 2θ is the scattering angle, and λ is the wavelength) by integrating the data in the complete isotropic scattering pattern. The intensities were normalized by the integrated intensity incident on the sample during the exposure and corrected for sample absorption and background scattering.

Infrared spectroscopy

Infrared spectra were recorded using a Spectrum 2000 FTIR spectrometer (Perkin-Elmer, USA) equipped with a Golden Gate single reflection ATR accessory (Specac, UK). Samples were dried for at least 72 h over silica gel before testing. Spectra were taken from 4000 to 600 cm^{-1} and averaged over 16 scans. Data was normalized to the total amide 1 band intensity from 1690 to 1600 cm^{-1}.

Structural modelling

Crystalline and nuclear magnetic resonance derived structures of potato proteins were taken from the Protein Data Bank[34]. The schematic ribbon diagrams showing changes in protein structure during processing of PPC were drawn with the help of I-TASSER[35], PyMOL Molecular Graphics System (version 1.3r1 edu, Schrödinger LLC, USA) and Adobe Illustrator.

Results and discussion

Tensile properties

The tensile properties of PPC based materials exhibit E-moduli and strain at break (ε_b) that are incongruent with previously examined thermoformed protein systems. E-modulus maintained a constant value within each glycerol level (15, 20 and 25%) over the applied pressing temperatures from 100 to 170 ^{o}C (Fig. 1, 2a). The general shapes of the tensile curves are consistent across the temperature range for each glycerol level (Fig. 1). Increased pressing temperature allowed the material to deform to higher stresses and strains along the typical curve for each glycerol level without having an impact on the curve shape. Attempts to press at higher temperatures (190 ^{o}C) resulted in untestable material due to thermal protein breakdown as indicated by the increase in soluble LMw protein at 5 minute pressing time (Fig. 3).

In previous thermoformed glycerol plasticized protein systems an increase in E-modulus with increased pressing temperature has been shown[19]. The previously observed increase in E-modulus with temperature was expected due to increased protein network density (cross-linking) as demonstrated through a decrease in protein solubility[20]. The statistical thermodynamic theory of cross linked macromolecular elastomers suggests a possible model for cross link density – E-modulus relationships[36]:

$$3(\text{E-modulus}) = G = NkT = \rho RT/M_c \qquad (1)$$

Where the shear modulus, G = 3 x E-modulus for incompressible solids[20], N = the number of network chains per unit volume, k = Boltzmann's constant, T = temperature, ρ = density, R = the gas constant and M_c = chain molecular weight between cross links.In the case of protein systems the situation appears to be more complex than indicated by equation 1 [20, 37]. When cross linked macromolecular elastomer theory has been applied to protein network swelling and mechanical properties, it was demonstrated that secondary structure and protein-protein interactions also have an effect on

network behaviour, not simply M_c[37]. In thermally processed PPC materials we found a decrease in protein extractability with temperature up to the minimum solubility at 150 °C (Fig. 3a). This suggests an increase in protein network development with temperature, up to 150 °C, but there is no corresponding increase in E-modulus over the same temperature range as is suggested by equation 1.

In the as-received PPC there is already low protein solubility and high HMw protein aggregates as a consequence of industrial processing[2] (Fig. 4). This indicates the existence of an insoluble protein network in the starting material before thermal processing. Heating the material during pressing increases the degree of networking, as indicated by changes in solubility and Mw (Fig. 3, 4), while no increase in E-modulus is observed when heated between 100 and 170 °C (Fig. 2). This behaviour is unusual for a thermally processed plasticized protein based material, and to our knowledge has not been previously reported.

The effect of glycerol content on E-modulus was found to be as expected for a plasticizer; higher glycerol levels decrease the E-modulus by reducing protein-protein interactions (Fig. 1, 2a). Glycerol levels were limited to 25% as glycerol migrated to the surface during conditioning at higher levels (i.e. at 30% glycerol, 50% RH, 23 °C). In other protein systems, e.g. wheat gluten[12] and soy protein isolate[38], glycerol levels as high as 40% have been successfully used.

Increasing press temperature positively influenced tensile strength (σ_{max}) and ε_b, resulting in increases up to pressing temperatures of 170 °C, prior to the onset of thermal breakdown (Fig. 1, 2b, c). As σ_{max} and ε_b are related to local deformation stability, such as crack initiation, the creation of a more cohesive network decreases the likelihood of a local failure. The development of the network through increased pressing temperature is seen in reduced overall solubility (Fig. 3a) and especially a reduction in HMw components in the extractable proteins, indicating the incorporation of HMw proteins into the cross linked network. The trend to higher σ_{max} at higher temperatures has been

previously observed in the wheat gluten protein based thermally-processed system[19] and in the heat treatment of cast soy protein films[21].

The glycerol level has an effect on the variation of σ_{max} and ε_b with temperature (Fig 2b,c). At higher temperatures (above 130 ^{o}C) the 15% glycerol material continues to increase in σ_{max} while the higher glycerol materials (20 and 25%) level off. It appears that this σ_{max} behaviour is due to the shape of the stress-strain curve, which forms a plateau at higher strains, while the 15% glycerol case has not reached the plateau before 170 ^{o}C (Fig. 1). Increasing pressing temperature increases ε_b up to the maximum testable processing temperature of 170 ^{o}C (Fig. 1, 2c). This contrasts with previous results in protein systems where ε_b decreases with increasing processing temperature[21, 22]. In terms of ε_b and σ_{max} the materials follow the same curve for each glycerol level with ε_b and σ_{max} varying with processing temperature as the materials proceed further up the tensile curve before failure (Fig. 1).

The overall tensile behaviour suggests an initial network formed at temperatures lower than 100 ^{o}C that remains dominant up to 170 ^{o}C. It is possible that to some extent this network is formed during initial protein production. Tensile failure, ε_b and σ_{max}, are controlled by the temperature of compression moulding and the changes in Mw distribution resulting from such processing. The E-modulus value in such a system appears to be dominated by the initial network as all materials behave the same in the low strain regime independent of processing temperature. The properties dependant on the expansion of the initial network, σ_{max} and $\varepsilon_{b,}$ are enhanced as network connectivity is strengthened by thermal processing.

Protein solubility and molecular weight distribution The as-received PPC contained a large proportion of HMw proteins eluting at low times (Fig. 4a). This HMw fraction in the as-received PPC is most likely due to protein-protein interactions formed during commercial protein coagulation as the reported proteins in untreated PFW are of low to medium Mw [3, 4]. In order to extract these HMw proteins sonication was required, 2000 rpm shaking with SDS-phosphate buffer was not sufficient to disrupt protein-protein interactions and induce solubility (Fig. 4). The interactions that

result from the formation of HMw protein aggregates and networks in the as-received PPC occurred at elevated temperatures and dilute aqueous acidic conditions. Film processing included only plasticizer and thermal treatment which may give rise to a different set of possible protein-protein interactions during compression moulding, allowing the expansion of the network previously formed during coagulation.

As the material is processed at increasing temperatures, the overall solubility decreases to a minimum at 150 ^{o}C (Fig. 3a). Above 150 ^{o}C an increase in the easily soluble proteins (extraction 1) eluting at the LMw end of the chromatogram indicates the formation of protein fragments from thermal degradation (Fig. 4). It should be noted that the HMw fraction decreases to almost 0 at 150 ^{o}C (Fig. 3c) and does not recover at higher temperatures undergoing thermal degradation. It appears that only small fragments are formed from thermal breakdown, not intermediate fragments (Fig. 4). The appearance of LMw fragments at 170 ^{o}C does not appear to have an adverse effect on σ_{max} and ε_b. At the highest temperature treatment (190 ^{o}C) the protein solubility increases to the same overall level as the original PPC, although with a shift to lower molecular weights (Fig. 4d).

Although SE-HPLC is a useful tool for examining the Mw of soluble proteins, the decrease in total soluble protein from 100 to 150 ^{o}C indicates the increasing incorporation of proteins in to the insoluble protein network (Fig. 3a) thereby influencing cross linking density. The effect of the incorporation of more protein into the network could be expected to increase N and decrease M_c (equation 1) through the higher fraction of participating chains and the formation of cross links, respectively. As there was no increase in the E-modulus with the change in level of soluble protein (Fig. 2a), the mechanical behaviour of the network either does not follow the statistical mechanics basis for equation 1[36] or its conditions are not met. The behaviour of the network can also be probed using solvent swelling experiments[20, 36, 37], see the discussion of water swelling below.

It may be expected that increased glycerol content would enhance protein mobility resulting in more opportunities to form a network as in the previously reported “chemical chaperone” effect[15]. In the

PPC case extractability and molecular weight data from SE-HPLC (Fig. 3, 4) exhibit little difference between glycerol levels. This indicates that the changes in σ_{max} and ε_b with glycerol level (Fig. 2c) are not due to glycerol effects on protein aggregation, but its effect on the shape of the stress-strain curve is through disrupting weak protein-protein interactions.

Changes in σ_{max} and ε_b can be correlated to changes in molecular weight. Figure 5a demonstrates the relationship between σ_{max} and the level of extractable HMw proteins. Lower amounts of extractable HMw proteins are found in higher strength PPC materials. It is believed that these proteins become insoluble by participating in the protein network, although their exact fate is not known. A log – log plot of ε_b vs. extractable HMw proteins (Fig. 5b) demonstrates that as the HMw proteins are captured by the network, ε_b increases. New thermally induced cross links interconnect the aggregated domains formed during PPC production increasing coherence of the network and increasing ε_b. Total soluble protein does not fit very well with the tensile data, possibly due to a population of LMw proteins that are resistant to participating in the network and LMw protein fragments from thermal degradation.

Water absorption

Water immersion of glycerol plasticized thermally processed PPC films resulted in swelling and weight gain which varied with pressing temperature (Fig. 6a). The mass gain decreased from 100 ^{o}C to 130-150 ^{o}C followed by an increase up to 190 ^{o}C in a similar way for all films. This behavior is similar to the overall protein solubility (Fig. 3a). Well developed theories based on statistical thermodynamics exist for the swelling of cross linked macromolecular networks, known as rubber elasticity[36]. Attempts have been made to apply rubber elasticity analysis to the swelling of protein systems[20, 37]. In the case of swelling wheat gluten based materials in water it was found that rubber elasticity did not adequately explain experimental data[20]. In the swelling of cross linked ovalbumin gels it was found that using 6M urea as a denaturing solvent removed secondary structure and led to behavior that was adequately described by rubber elasticity theory[37].

Whatever the specific relationship between rubber elasticity and swelling in protein based systems, both studies suggest that lower swelling indicates a higher degree of cross linking. A higher degree of cross linking should also result in a higher value of E-modulus, although the exact nature of this relationship is also unclear. In our case the variation in swelling with film processing temperature suggests changes in cross linking (Fig. 6a), but there is no associated change in the E-modulus in the same temperature range (Fig. 2a).[20]

The dry mass of the films after swelling was also affected by processing temperature. Mass loss decreased from 100 ^{o}C to the minimum at 150-170 ^{o}C followed by an increase at 190 ^{o}C (Fig. 6b).In the 100 to 170 ^{o}C range solubility decreases as cross-linking increases while above 170 ^{o}C thermal protein fragmentation begins (Fig. 3b, 4d). The differences between mass loss in water (Fig. 6b) and total protein extraction with SDS buffer (Fig. 3a) may be due to the action of SDS on weak interactions and the energy applied during extraction in the form of shaking and sonication.

Glycerol level affected mass loss significantly but showed only a minor effect on mass gain, indicating that glycerol molecules are already occupying positions in the network that otherwise could have been taken up by water (Fig. 6a). In the case of mass loss (Fig. 6b), previous work has shown that on immersion glycerol is dissolved into the immersion water[20]. On drying it is expected that the films will lose their glycerol mass along with the dissolved components, resulting in the observed glycerol effect.

Protein secondary structure through IR absorption

IR absorption was used to examine the changes in the amide 1 region (1700-1600 cm^{-1}) where C=O vibrations are a sensitive indicator of secondary protein structure, correlating well with other methods [39]. Changes in secondary structure as revealed through IR absorption have been used to examine the development of protein configuration due to processing in protein based materials and

its effect on protein aggregation, film formation and material processing in a number of studies [23, 24, 40-43].

The initial heating step from as- received PPC to material pressed at 100 °C showed an increase in β-sheet content as indicated by the increase in the FTIR spectrum around 1625 cm^{-1} [23](Fig. 7a). IR spectroscopy of pressed samples showed little development in the amide 1 region (1690-1600 cm^{-1}) at increasing processing temperatures from 100 to 150 °C indicating a lack of further development in secondary structure (Fig. 7a). From 170 to 190 °C a change in secondary structure was again seen (Fig. 7a,b), likely due to thermal damage causing a loss of protein integrity. The ratio of intensity at 1625cm^{-1} (β-sheet region[23, 24, 40-43]) to 1652 cm^{-1} (α-helix/disordered region[23, 24, 40-43]) (Fig. 7b) indicates a large change in structure on initial heating to 100 °C, followed by minor changes to the secondary structure from 100 to 150 °C, with a decrease in the ratio of β-sheet to α-helix/disordered at higher temperatures. The effect of glycerol on structure (Fig. 7b,c) is also minor, except for 25% glycerol at 150 °C where increased plasticization appears to have pushed the structure towards the changes that occur at 170 °C at all glycerol levels.

The literature contains examples where it is suggested that mechanical property development in protein based material is at least in part due to changes in secondary structure [23, 40, 41, 43]. In our case little change in secondary structure accompanies changes in σ_{max} and ε_b, while changes in extractable HMw protein correlate to σ_{max} and ε_b changes (Fig. 5) indicating that in this case secondary structural changes are not important in mechanical property development from 100 to 170 °C.

Small angle X-ray scattering

In contrast to the IR absorption data, SAXS data shows clear changes in morphology with increasing pressing temperature (Fig. 8, Table 1). The as-received PPC powder contains no SAXS scattering peaks, while films pressed at 100 to 150 °C show two peaks with correlation distances[44, 45], the average distance between domains, of 75-95 Å(d_2) and 44 to 48Å (d_3) (Fig 8, Table 1). Interestingly,

at 130 °C the d_2 peak is more pronounced than at other temperatures. An additional peak, d_1, appears at 150, 170 and 190 °C (very weak at 150 °C, 195 and 192Å at 170 and 190 °C, respectively). The position of d_2 and d_3 remains fairly constant from 150 to 190 °C.

Although scattering intensities clearly change in the thermoformed films, the peak position relationships do not correspond to any well defined long range ordered morphology (Table 1) as have been seen previously for thermoformed WG-based materials, e.g. hexagonal or tetragonal structures[15, 18]. There is some change in peak position with both pressing temperature (Fig. 8a) and glycerol content (Fig. 8b), although these changes are not correlated with each other. Thus, the peaks d_1, d_2 and d_3 represent the behaviour of different correlation distances in present the system. The appearance of d_1 at higher temperatures corresponds to the occurrence of LMw fragments in SE-HPLC (Fig. 3b and 4d) and may be due to the presence of protein fragments that have become free to reorganize.

Changes in glycerol content appear to have little effect on the d-spacing found in the system at 170 °C, with the increased glycerol slightly shifting peak position to lower spacing (Fig. 8b, Table 1). It may be expected that increased glycerol content would swell the structure. Increased glycerol content causes d_2 to shift to higher distances while d_3 shifts to smaller distances (Fig. 8b, Table 1). This indicates that glycerol is not evenly distributed on the scale probed by SAXS. A schematic representation (Fig. 9) shows a possible visualization of the morphological changes occurring from the processing of PFW to a developed network structure in thermoformed PPC film. The PFW contains the major protein groups, patatin and protease inhibitors (Fig. 9a), as described earlier in the manuscript. Upon industrial processing of PFW to PPC the structure of the proteins are denatured and refold as a cross linked network without any specific structure developing (Fig. 9b) as shown by solubility (Fig 3.), IR (Fig. 7) and SAXS (Fig. 8) results. Thermoforming to 170 °C (Fig. 9c) results in an increase in protein cross linking (Fig. 3), the development of β-sheet structure

(compared to unpressed PPC) (Fig.7) and the appearance of independent characteristic distances as observed in SAXS (Fig. 8).

Conclusions

Commercially available PPC, plasticized with glycerol and thermally processed, resulted in protein-based materials with unusual polymerization and tensile properties. Unexpectedly, E-modulus was only affected by glycerol level and did not change with processing temperature, a different behavior as related to previous reports on protein-based systems. Protein secondary structure was also unaffected by processing temperature, despite changes in protein solubility with temperature, indicating a possible cause for the constant E-modulus. The as-received PPC showed the presence of polymerized proteins before the thermoforming of films. This initial protein network may also be responsible for the constant E-modulus by providing a basic level of network interconnectivity across all processing temperatures. A decrease in the extractable HMw fraction of the protein brought on by thermal processing corresponded with an increase in both σ_{max} and ε_b. An increase in σ_{max} with temperature followed theories for cross-linking of proteins that have been previously developed, while the increase in ε_b with temperature did not. The reason for this discrepancy might be that new thermally induced cross links are interconnecting the aggregated domains formed during PPC production increasing network cohesion and thus ε_b.

Acknowledgements

The authors would like to thank Joakim Ekelöf and Lyckeby Starch AB for providing the commercial potato protein concentrate, Maria Luisa Prieto-Linde for technical assistance, research school and research program Trees and Crops for the Future (TC4F), Ventenskapsrådet (VR), Vinnova, Partnerskap Alnarp, Bioraf Öresund and project ICON for support. MAX IV Laboratory is acknowledged for the beamtime provided under proposal 20140273.

399

References

1. S. Løkra, M. H. Helland, I. C. Claussen, K. O. Strætkvern and B. Egelandsdal, *LWT-Food Sci. Technol.*, 2008, **41**, 1089-1099.
2. D. Knorr, *J. Food Sci.*, 1980, **45**, 1183-1186.
3. A. M. Pots, H. Gruppen, R. van Diepenbeek, J. J. van der Lee, M. A. J. S. van Boekel, G. Wijngaards and A. G. J. Voragen, *J. Sci. Food Agric.*, 1999, **79**, 1557-1564.
4. L. Pouvreau, H. Gruppen, S. Piersma, L. Van den Broek, G. Van Koningsveld and A. Voragen, *J. Agric. Food Chem.*, 2001, **49**, 2864-2874.
5. M. Friedman, G. M. McDonald and M. Filadelfi-Keszi, *Crit. Rev. Plant Sci.*, 1997, **16**, 55-132.
6. D. C. Rees and W. N. Lipscomb, *J. Mol. Biol.*, 1982, **160**, 475-498.
7. T. J. Rydel, J. M. Williams, E. Krieger, F. Moshiri, W. C. Stallings, S. M. Brown, J. C. Pershing, J. P. Purcell and M. F. Alibhai, *Biochemistry*, 2003, **42**, 6696-6708.
8. E. M. Meulenbroek, E. A. Thomassen, L. Pouvreau, J. P. Abrahams, H. Gruppen and N. S. Pannu, *Acta Crystallogr., Sect. D: Biol. Crystallogr.*, 2012, **68**, 794-799.
9. A. R. Green, M. S. Nissen, G. M. Kumar, N. R. Knowles and C. Kang, *The Plant Cell,* 2013, **25**, 5043-5052.
10. M. Friedman, *J. of Agric. Food Chem.*, 1997, **45**, 1523-1540.
11. E. DellaMonica, E. Strolle and P. McDowell, *Anal. Biochem.*, 1976, **73**, 274-279.
12. M. Gällstedt, A. Mattozzi, E. Johansson and M. S. Hedenqvist, *Biomacromolecules*, 2004, **5**, 2020-2028.
13. H. J. Kang and S. C. Min, *LWT-Food Sci. Technol.*, 2010, **43**, 903-909.
14. I. Rombouts, B. Lagrain, J. A. Delcour, H. Türe, M. S. Hedenqvist, E. Johansson and R. Kuktaite, *Ind. Crops Prod.*, 2013, **51**, 229-235.
15. F. Rasheed, W. R. Newson, T. S. Plivelic, R. Kuktaite, M. S. Hedenqvist, M. Gällstedt and E. Johansson, *RSC Adv.*, 2014, **4**, 2051-2060.
16. B. Cuq, F. Boutrot, A. Redl and V. Lullien-Pellerin, *J. Agric. Food Chem.*, 2000, **48**, 2954-2959.
17. W. Newson, R. Kuktaite, M. Hedenqvist, M. Gällstedt and E. Johansson, *J. Am. Oil Chem. Soc.*, 2013, **90**, 1229-1237.
18. R. Kuktaite, T. S. S. Plivelic, Y. Cerenius, M. S. Hedenqvist, M. Gällstedt, S. Marttila, R. Ignell, Y. Popineau, O. Tranquet, P. R. Shewry and E. Johansson, *Biomacromolecules*, 2011, **12**, 1438-1448.
19. S. Sun, Y. Song and Q. Zheng, *Food Hydrocolloids*, 2008, **22**, 1006-1013.
20. S. Domenek, L. Brendel, M. H. Morel and S. Guilbert, *Biomacromolecules*, 2004, **5**, 1002-1008.
21. A. Gennadios, V. Ghorpade, C. L. Weller and M. Hanna, *Trans. ASAE*, 1996, **39**, 575–579.
22. S.-W. Cho, H. Ullsten, M. Gällstedt and M. S. Hedenqvist, *J. Biobased Mater. Bioenergy*, 2007, **1**, 56-63.
23. H. Türe, M. Gällstedt, R. Kuktaite, E. Johansson and M. S. Hedenqvist, *Soft Matter*, 2011, **7**, 9416-9423.
24. C. Mangavel, J. Barbot, Y. Popineau and J. Guéguen, *J. Agric. Food Chem.*, 2001, **49**, 867-872.
25. A. Brandenburg, C. Weller and R. Testin, *J. Food Sci.*, 1993, **58**, 1086-1089.
26. T. Yoshino, S. Isobe and T. Maekawa, *J. Am. Oil Chem. Soc.*, 2002, **79**, 345-349.
27. M. Prochoń, A. Przepiórkowska and Y.-H. Tshela Ntumba, *ISRN Polym. Sci.*, 2012, **2012**.
28. B. Lagrain, B. Goderis, K. Brijs and J. A. Delcour, *Biomacromolecules*, 2010, **11**, 533-541.
29. C. R. Álvarez-Chávez, S. Edwards, R. Moure-Eraso and K. Geiser, *J. Cleaner Prod.*, 2012, **23**, 47-56.
30. M. Pommet, M.-H. Morel, A. Redl and S. Guilbert, *Polymer*, 2004, **45**, 6853-6860.
31. ASTM Standard D 638-86, American Society for testing and Materials, Philadelphia, 1986.

32. W. R. Newson, R. Kuktaite, M. S. Hedenqvist, M. Gällstedt and E. Johansson, *J. Agric. Food Chem.*, 2014, **62**, 6707-6715.
33. A. Labrador, Y. Cerenius, C. Svensson, K. Theodor, and T. Plivelic, *J. Phys.: Conf. Ser.*, 2013, **425**, 7, 072019.
34. H. M. Berman, J. Westbrook, Z. Feng, G. Gilliland, T. Bhat, H. Weissig, I. N. Shindyalov and P. E. Bourne, *Nucleic Acids Res.*, 2000, **28**, 235-242.
35. J. Yang, R. Yan, A. Roy, D. Xu, J. Poisson and Y. Zhang, *Nat. Methods*, 2015, **12**, 7-8.
36. L. R. G. Treloar, *The Physics of Rubber Elasticity*, Oxford University Press, 1975.
37. F. Van Kleef, J. Boskamp and M. Van den Tempel, *Biopolymers*, 1978, **17**, 225-235.
38. A. Gennadios, J. Rhim, A. Handa, C. Weller and M. Hanna, *J.Food Sci.*, 1998, **63**, 225-228.
39. D. M. Byler and H. Susi, *Biopolymers*, 1986, **25**, 469-487.
40. T. O. Blomfeldt, R. T. Olsson, M. Menon, D. Plackett, E. Johansson and M. S. Hedenqvist, *Macromol. Mater. Eng.*, 2010, **295**, 796-801.
41. F. Muneer, M. Andersson, K. Koch, C. Menzel, M. S. Hedenqvist, M. Gällstedt, T. S. Plivelic and R. Kuktaite, *Biomacromolecules*, 2015.
42. M. Subirade, I. Kelly, J. Guéguen and M. Pézolet, *Int. J. Biol. Macromol.*, 1998, **23**, 241-249.
43. M. Oliviero, E. Di Maio and S. Iannace, *J. Appl. Polym. Sci.*, 2010, **115**, 277-287.
44. H. Huang, and G. L. Wilkes, Polym. Bull., 1987, **18**, 455-462.
45. K. Polat, I. Orujalipoor, S. İde, and M, Şen, J. Polym. Eng., 2015, **35**, 151-157.

467 **Table 1** Peak spacing from small angle X-ray scattering of PPC based materials.
468
469
470

Pressing Temperature (^{o}C)	glycerol (%)	d_1 (Å)	d_2 (Å)	d_3 (Å)
constant glycerol, varying temperature				
100	25	-	75.2	44.6
120	25	-	94.9	44.6
130	25	-	85.8	44.2
150	25	-	95.3	48.5
170	25	195	93.5	47.7
190	25	192	96	48.5
constant temperature, varying glycerol				
170	15	197	87.1	49.9
170	20	191	90.4	47.8
170	25	195	93.5	47.7

471

Figure 1. Representative tensile behaviour of thermoformed films of glycerol plasticized potato protein concentrate.

Figure 2. Average tensile behaviour of thermoformed potato protein plastics, a) Young's modulus (E-modulus) vs. thermoforming temperature, b) maximum stress (σ_{max}) vs. thermoforming temperature, c) strain at break (ε_b) vs. thermoforming temperature. Error bars represent standard deviation.

Figure 3. Protein solubility as measured by absorption at 210nm in SE-HPLC, a) total integrated absorption vs. pressing temperature, b) absorption of low molecular weight (LMw) protein vs. pressing temperature, c) absorption of high molecular weight (HMw) protein vs. pressing temperature. All integration s are the sum of 3 extractions. Elution intervals; HMw fraction 8-14 minutes, LMw fraction 14-30 minutes. Absorption normalized to total integrated signal for as-received potato protein concentrate. Error bars denote standard deviation.

Figure 4. Changes in representative SE-HPLC chromatograms with thermal processing, a) as-received potato protein concentrate (PPC), PPC with 25% glycerol pressed at; b) 100 ^{o}C, c) 150 ^{o}C, d) 190 ^{o}C. All extractions in SDS-phosphate buffer; extraction 1 - shaking 5 minutes, extraction 2 - 30s sonication, extraction 3 - 30 +60 seconds sonication.

Figure 5. Relationships between Mw and tensile properties, a) effect of soluble HMw protein on strength (σ_{max}), b) effect of soluble HMw protein content on strain at break (e_b) (note the log-log axes). Error bars denote standard deviation.

Figure 6. Effect of 24hr water immersion on PPC based materials, a) effect of processing temperature on mass gain due to swelling, b) mass loss due to soluble components and glycerol migration. Error bars denote standard deviation.

Figure 7. ATR-FTIR spectra of thermoformed potato protein; a) effect of increasing temperature, glycerol content 25%, b) ratio of absorbtion at 1623cm^{-1} (β-sheet) to 1652cm^{-1} (α-helix/disordered)

versus temperature (error bars denote one standard deviation, heights are baseline corrected from 1700 to 1580cm^{-1}), c) effect of increasing glycerol content, samples pressed at 170 ^{o}C.

Figure 8. Small angle X-ray scattering of thermoformed potato protein concentrate based materials; a) effect of increasing temperature in pressed samples at a glycerol content of 25%, b) effect of increasing glycerol content in samples pressed at 170 ^{o}C.

Figure 9. Schematic representation of potato protein processing and resulting structural rearrangement: a) native proteins in potato fruit water (PFW), 1; Potato carboxypeptidase A[6] (Protein Data Base (PDB) ID: 4CPA), 2; patatin[7] (PBD ID: 1OXW), 3; potato serine protease inhibitor[8] (PDB ID: 3TC2), 4; potato multicystatin[9] (PDB ID: 4LZ1), b) denaturation during industrial processing of PFW to potato protein concentrate (PPC), c) structural changes occurring during thermoforming of PPC based film (170 ^{o}C, 30% glycerol) as observed in FT-IR, d) schematic representation of structure from SAXS. Note: b, and c were produced in I-TASSER and displayed in PyMOL as an illustration of secondary structural changes and are schematic representations only, they do not reflect actual PPC conformation.

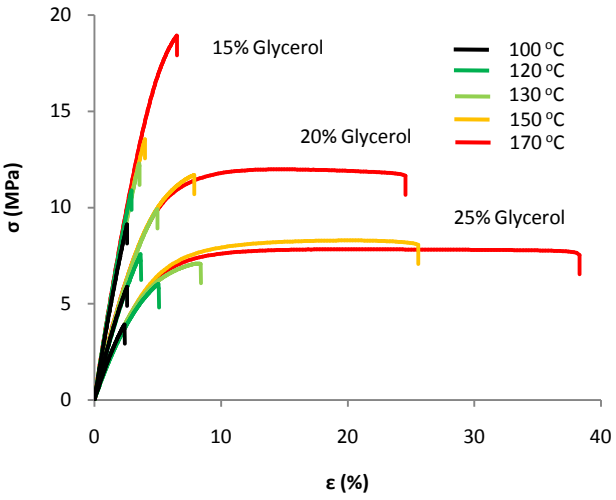

Figure 1

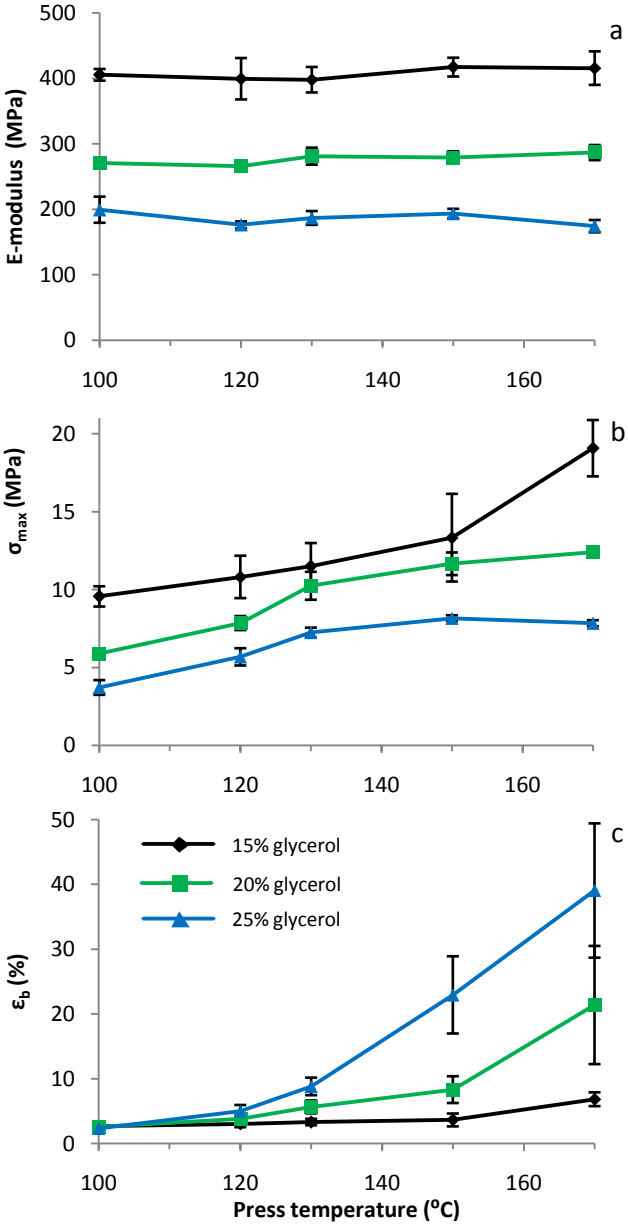

Figure 2

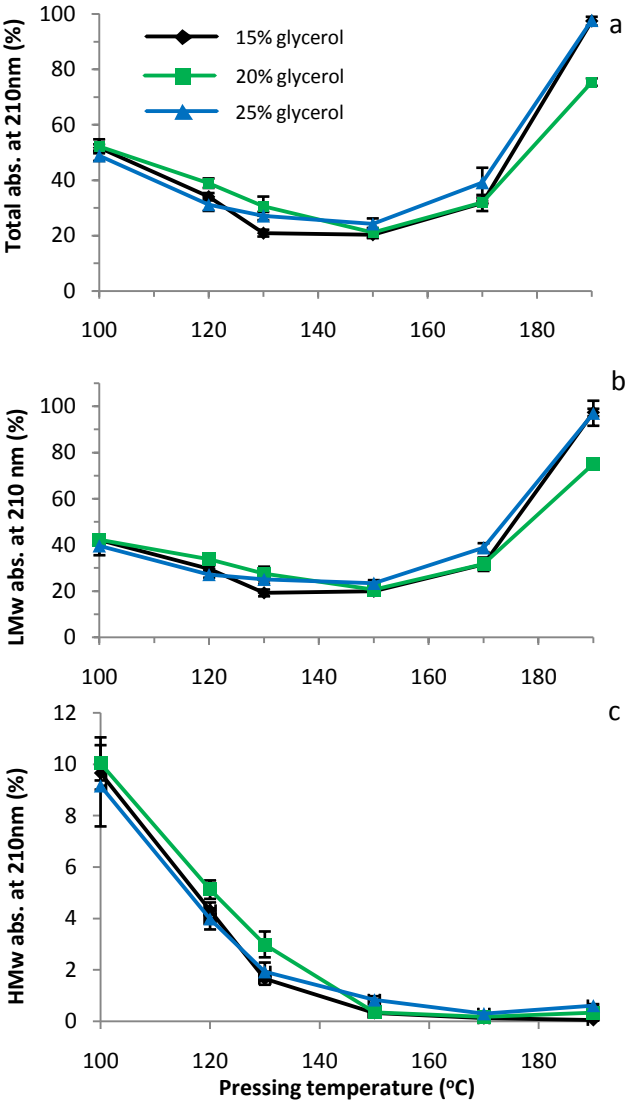

Figure 3

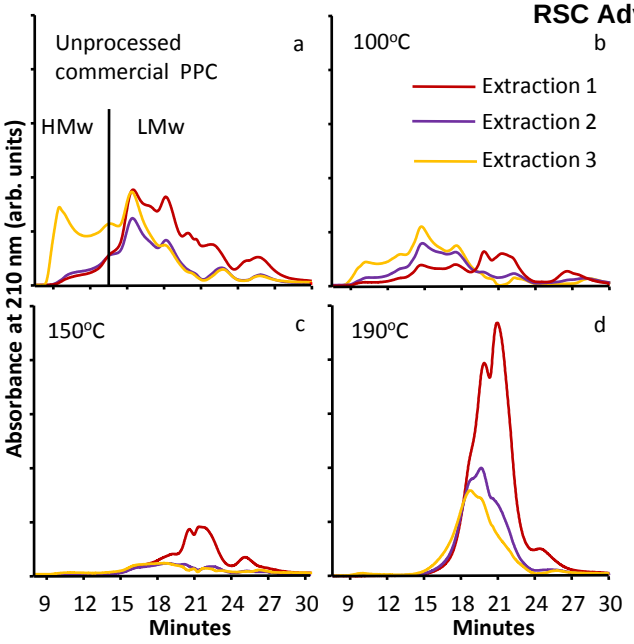

Figure 4

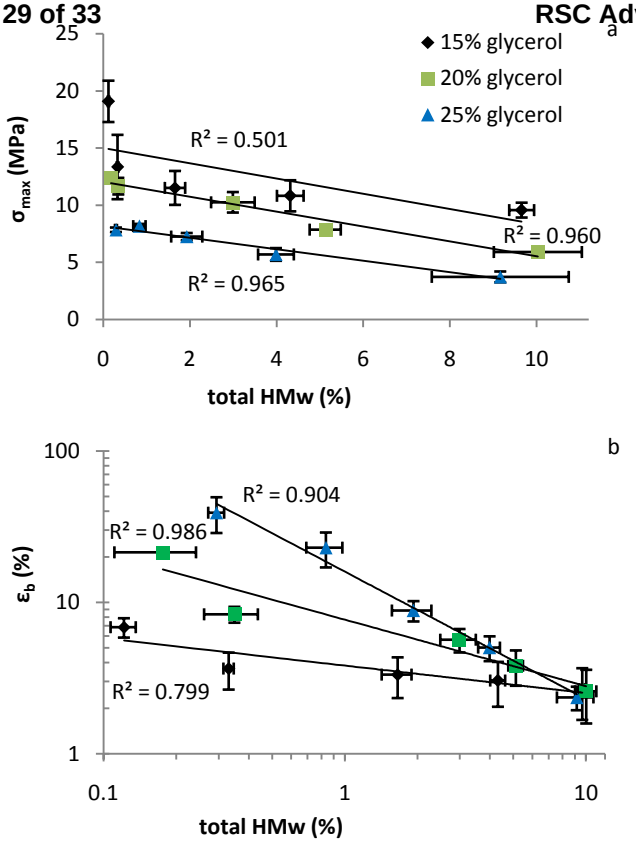

Figure 5

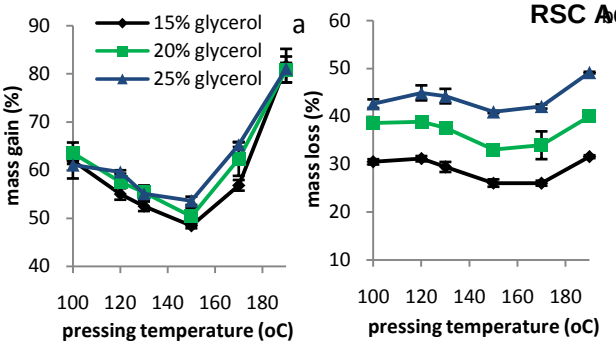

Figure 6

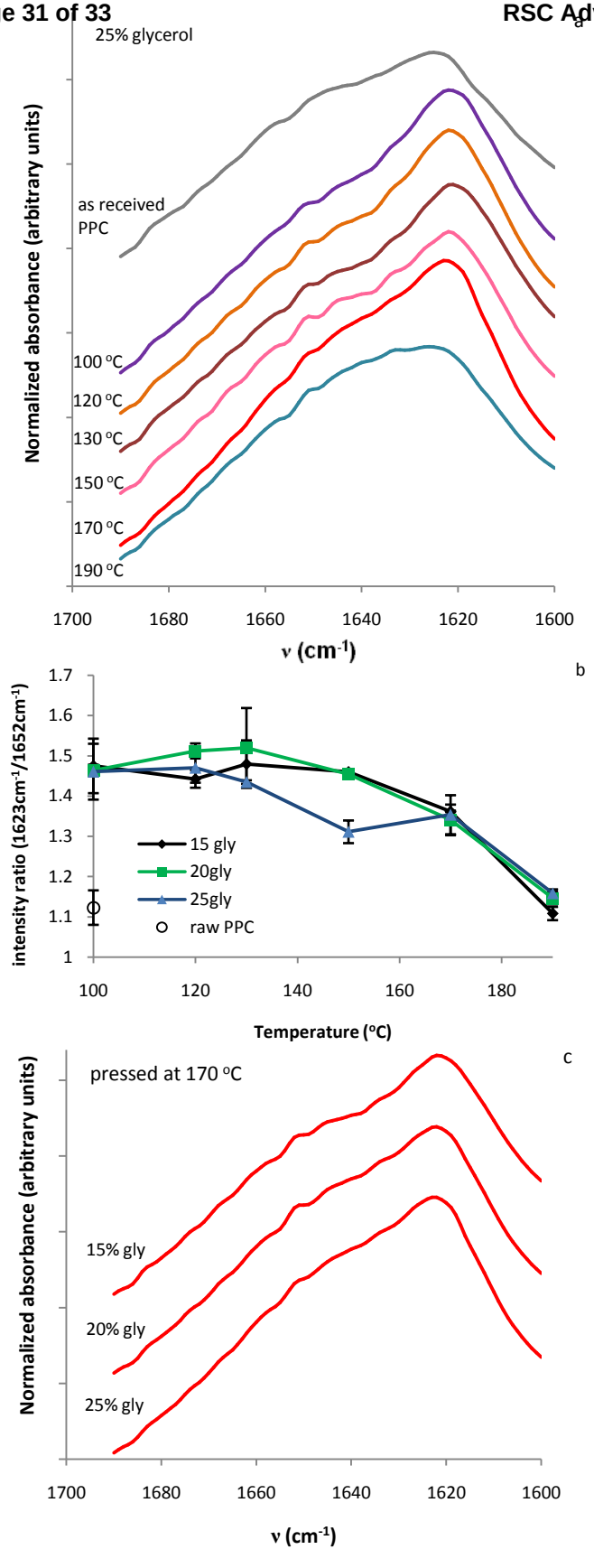

Figure 7

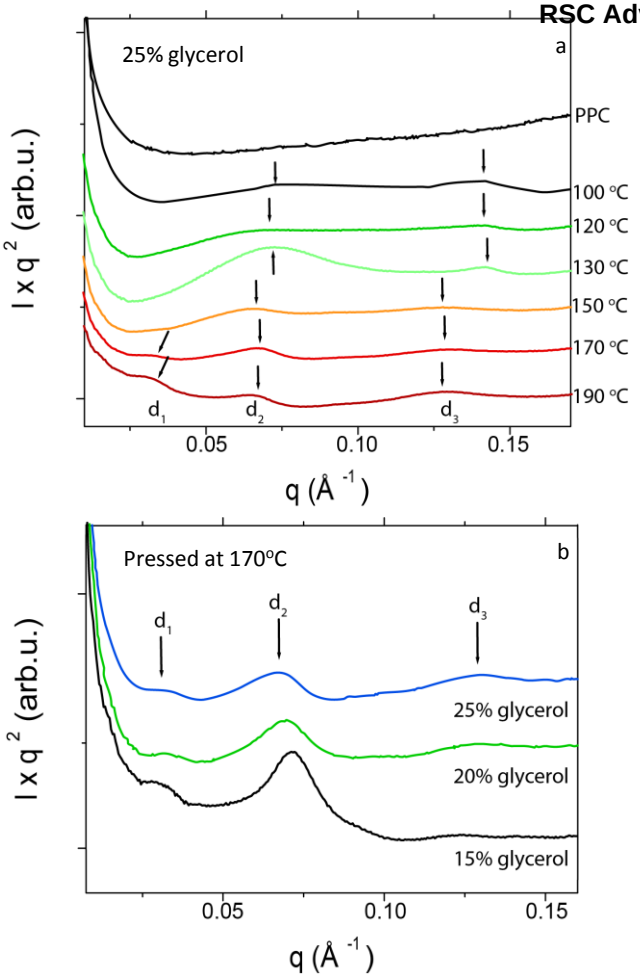

Figure 8

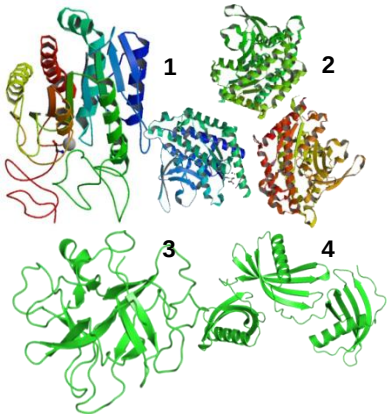

a) Proteins in potato fruit water
1. PCP A, 2. Patatin, 3. PSPI, 4.PMC

Industrial processing

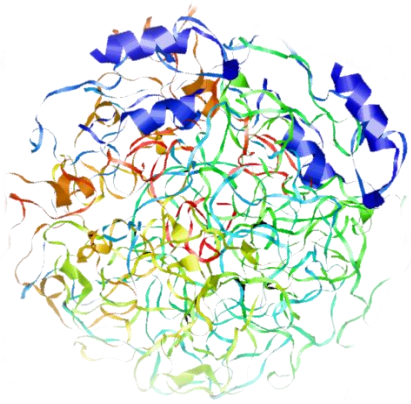

b) Denatured proteins in PPC

Film processing

Resulting structure

SAXS

FT-IR

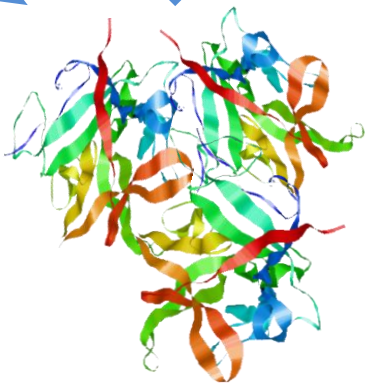

c) Protein structural re-arrangement in thermoformed PPC film

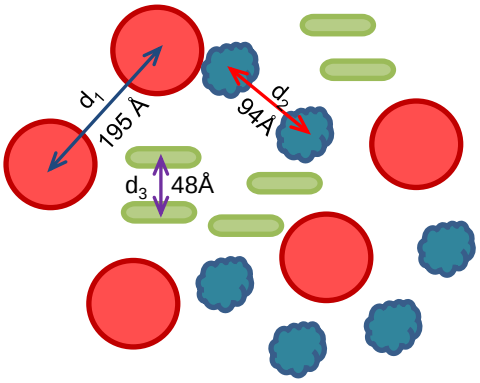

d) Schematic representation of scattering objects in thermoformed plasticized film as observed in SAXS

Figure 9